Jurnal Teknologi

Full Paper

SIMULATION STUDY ON THE SPRAY CHARACTERISTICS OF PALM OIL DIESEL BLEND BY USING DISCRETE PHASE MODEL

M. A. Subri[a], S. N. Soid[a,*], I. A. Azid[a], M. H. H. Ishak[b]

[a]Universiti Kuala Lumpur Malaysian Spanish Institute, Kulim Hi-Tech Park, 09090 Kulim, Kedah, Malaysia
[b]School of Aerospace Engineering, Universiti Sains Malaysia, Engineering Campus, 14300 Nibong Tebal, Penang, Malaysia

Article history
Received
1 May 2024
Received in revised form
21 July 2025
Accepted
13 August 2025
Published Online
30 April 2026

*Corresponding author
shahrilnizam@unikl.edu.my

Graphical abstract

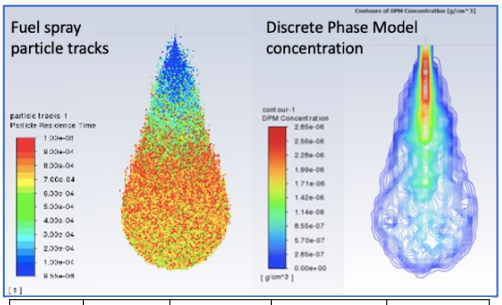

Fuel	Injection pressure (MPa) and Nozzle Size (mm)	Average tip penetration / % different	Average cone angle / % different	SMD / % different
Diesel	160/ 0.18	65.10 mm / -	38.71° / -	9.55 x 10^{-9} mm / -
P20	200/ 0.22	77.00 mm / 15.46 % longer	41.40° / 6.50 % wider	6.16 x 10^{-9} mm / 35.51 % smaller
P40	200/ 0.20	91.48 mm / 28.84 % longer	30.08° / 28.67 % narrower	1.14 x 10^{-8} mm / 19.65 % larger
P60	200/ 0.20	111.07 mm / 41.38 % longer	23.74° / 63.09 % narrower	1.62 x 10^{-8} mm / 69.41 % larger
P80	200/ 0.20	117.27 mm / 44.49 % longer	18.12° / 113.66 % narrower	2.17 x 10^{-8} mm / 126.91 % larger
P100	200/ 0.20	124.61 mm / 47.76 % longer	16.82° / 130.10 % narrower	2.38 x 10^{-8} mm / 149.38 % larger

Abstract

Palm oil diesel blend is being promoted as a practical and greener alternative to fossil-based fuels such as petrol and diesel. To be utilised in diesel engines, this biofuel, also referred to as biodiesel, is frequently mixed in different proportions with petroleum-based diesel fuel. However, the usage of biofuel degrades the engine performance due to its poor spray characteristics and atomization. The spray characteristics and atomization of fuel are important aspects during the combustion process, as they affect the combustion efficiency and pollution emissions. In this study, the fuel spray model of palm oil diesel blend (PODB) was developed using Ansys Fluent software. The initial model was developed based on the diesel injection process and then was used for palm oil and its blend with diesel. Further investigations were conducted on the effects of nozzle hole size, injection pressure, and blend ratio. The validation of the developed spray model was conducted by comparing it to previous experimental and simulation studies by other researchers. The percentage of error was found to be at about 8.25 % and 10.64 % compared to experimental and simulation studies, respectively. From the analysis, it was found that higher density and viscosity PODB would produce longer tip penetration, a narrower cone angle, and a larger Sauter mean diameter (SMD). A significant effect was shown where higher injection pressure and larger nozzle hole size would produce longer tip penetration and smaller SMD. For PODB, the injection pressure and nozzle hole size were suggested to be increased by about 25 % compared to the standard condition for diesel.

Keywords: Spray characteristics, atomization, droplet size, Sauter mean diameter, palm oil diesel blend

Abstrak

Campuran diesel minyak sawit merupakan alternatif yang praktikal dan lebih hijau kepada bahan api berasaskan fosil seperti petrol dan diesel. Untuk digunakan dalam enjin diesel, biofuel ini, juga dirujuk sebagai biodiesel, sering dicampur dalam perkadaran yang berbeza dengan bahan api diesel. Walau bagaimanapun, penggunaan biofuel merendahkan prestasi enjin kerana ciri semburan dan pengabusannya yang lemah. Ciri-ciri semburan dan pengabusan bahan api adalah aspek penting semasa proses pembakaran kerana ia mempengaruhi kecekapan pembakaran dan pelepasan pencemaran. Dalam kajian ini, model semburan bahan api campuran diesel minyak sawit (PODB) telah dibangunkan menggunakan perisian Ansys Fluent. Model awal dibangunkan berdasarkan proses suntikan

bahan api diesel, dan kemudian digunakan untuk minyak sawit dan campurannya dengan diesel. Kajian lanjut telah dijalankan ke atas kesan saiz lubang muncung, tekanan suntikan, dan nisbah campuran. Pengesahan model semburan yang dibangunkan telah dijalankan dengan membandingkan kerja eksperimen dan simulasi sebelumnya oleh penyelidik lain. Peratusan ralat didapati masing-masing kira-kira 8.25% dan 10.64% berbanding kerja-kerja eksperimen dan simulasi. Daripada analisis, didapati ketumpatan dan kelikatan PODB yang lebih tinggi akan menghasilkan semburan yang lebih panjang dan sudut kon yang lebih kecil serta Sauter min diameter (SMD) yang lebih besar. Kesan ketara ditunjukkan di mana tekanan suntikan yang lebih tinggi dan saiz lubang muncung yang lebih besar akan menghasilkan panjang semburan yang lebih jauh dan SMD yang lebih kecil. Untuk PODB, tekanan suntikan dan saiz lubang muncung dicadangkan dinaikkan pada kira-kira 25% dibandingkan dengan keadaan standard untuk diesel.

Kata kunci: Ciri semburan, pengabusan, saiz titisan, Sauter min diameter, campuran diesel minyak sawit

1.0 INTRODUCTION

Malaysia's immense supply of palm oil provides a tremendous opportunity to be used as an alternative and renewable energy resource for diesel engines. However, due to different physical properties of the fuel, engine performance degrades due to its poor injection process. Therefore, the fuel injection process needs to be controlled, as the improvement of spray characteristics is vital for engine performance [1], especially for gas emissions and combustion efficiency. Studies on fuel spray performance measurement techniques [2] and the atomization and spray characteristics of biofuels were reviewed [3], [4], [5], [6] in previous publications. As of today, numerous studies have been published related to this area. Most of the studies were conducted either experimentally or numerically or both, with the aim to obtain the correct configuration for fast development of the fuel spray process. Faster fuel spray development is shown by longer tip penetration, wider cone angle, and smaller droplet size.

Based on previous studies, it was found that higher injection pressure would produce longer tip penetration [7], [8], [9], [10], [11], [12], [13]. Tip penetration would also increase with the decreasing of chamber pressure due to the less resistance for the fuel during the injection process [7], [11], [12], [13]. The density and viscosity of fuel also influence the tip penetration development. Higher density and viscosity fuel will produce longer tip penetration due to the momentum carried out by the liquid fuel [12]. Meanwhile, for higher ambient temperatures inside the combustion chamber, shorter penetration lengths are produced due to air with higher temperatures having lower density compared to cooler air [11]. The fuel's density, characteristics, and nozzle size have an impact on the cone angle [9], [14].

A previous study also found the smaller nozzle size will produce shorter tip penetration [8]. This happens due to the smaller nozzle size, which produces higher resistance for the fluid to pass through. Furthermore, cone angle decreases with increasing velocity and tip penetration [13]. The cone angle will also decrease with increasing viscosity and density [12]. However, the influence of injection pressure towards the cone angle is modest between 80 and 250 MPa injection pressures for diesel fuel [15]. In the case of biofuel, some studies were carried out by utilising computational fluid dynamic software such as Ansys Fluent [16], [17] and Ansys Forte [18] since fuel spray characteristics studies involved the fluid flow and thermal analysis. A study by Khalid *et al.* [16] showed that longer tip penetration and a narrow cone angle were produced by higher viscosity and density fuel. Meanwhile, another study by Kafrawi and Bari [18] on the palm-based biodiesel showed that longer tip penetration and larger droplet size were produced by fuel that had higher viscosity, density, and molecular weight.

The development of fuel spray and atomization using simulation methods is still being studied by many researchers, as the spray characteristics of fuel are still of research interest due to the unique conditions of engines with regard to fuel characteristics such as viscosity and surface tension. The study on atomization has a significant impact, especially on understanding fuel evaporation and droplet formation. Thus, the injection process can be controlled to ensure complete combustion and lower the emission products. In the case of palm oil diesel blend, recent studies conducted focus on the performance of the engine in terms of power output and emissions. The engine performance and its emissions depend on the combustion performance, and it can be improved by controlling the fuel injection process, especially on the Sauter mean diameter. The purpose of this study is to examine the palm oil diesel blend (PODB) spray properties in terms of tip penetration, cone angle, and Sauter mean diameter. The optimum configuration for PODB based on different injection pressures and nozzle sizes was also studied.

2.0 METHODOLOGY

The fuel injection system's function is to supply fuel to the engine cylinders and to carefully monitor the injection durations, the atomization of the fuel, and other parameters. Very high injection pressures are achieved by modern injection systems and advanced electronic control methods. In this study, a six-hole diesel fuel injector (Delphi CRDI 6650170321) used for Ssangyong Rexton, as shown in Figure 1, was chosen for the analysis. As measured by the actual diesel fuel injector, each injector nozzle was 1.23 mm in length and 0.18 mm in diameter. Table 1 shows the injector specification, and Table 2 demonstrates the simplified geometry of the combustion chamber used in this study.

Figure 1. Delphi CRDI 6650170321 fuel injector

Table 1 Fuel injector specification

Model	Delphi CRDI 6650170321
Working Pressures	30-180 MPa
Number of nozzles	6
Size of nozzle	0.18 mm

Table 1 Simplified Rectangular Volumetric Combustion Chamber Geometry for Ansys Study

Width	40 mm
Depth	40 mm
High	140 mm

A six-hole diesel fuel injector formed the basis for the CAD model's development. However, only one hole out of six nozzles was modelled to reduce computing time.

2.1 Modelling Step and Governing Equations

The simulation setup for Ansys Fluent version 23.2 CFD software used in this study is shown in Table 3. The setups used are the pressure-based type, the absolute velocity formulation, and transient time as the solver types. In this case, the projection method is the algorithm used by the pressure-based solver. The projection approach satisfies the velocity field's mass conservation (continuity) condition by solving a pressure equation. The pressure, which is derived from the continuity and momentum equations, corrects the velocity field to fulfil the pressure equation. The mixture model was used to clarify the multiphase flow, considering the uniform mixing of the liquid and vapour phases. To determine the right number of elements for the analysis, a mesh sensitivity study was conducted. For the mesh sensitivity study, quad and tetrahedron meshes were tested at various numbers of elements ranging from 300,000 to 2,000,000. From the analysis, it was found that the quad mesh and 1,500,000 number of elements converged at the shortest time and were selected for this study.

Table 3 Solver, Turbulence Model and Phase Model

Classification	Setting of spray simulation
Flow type	Incompressible
Solver	Pressure-Based Type Absolute Velocity Formulation Transient Time
Turbulence model	Standard k-omega (2 equations) Standard Wall Functions
Phase model	Discrete Phase Model
Type of mesh	Quad, Tetrahedron
Number of elements	300 000, 600 000, 900 000, 1 000 000, 1 500 000, 1 800 000 and 2 000 000.
Time step	1e-5
No time step	100

The continuity, momentum, and energy equations are governing the fuel's continuous flow from the injector, which solves the Navier-Stokes equations. Iterations are used during the process of solving governing equations so that all equations are solved until the solution converges. In the setup tree for the model, viscous was selected. Then the standard $k-\omega$ was selected as the viscous model. The standard $k-\omega$, which encompassed modifications of low-Reynolds number effects, compressibility, and shear flow spreading, was chosen for the turbulence model. The standard $k-\omega$ is an empirical model based on model transport equations for the specific dissipation rate and turbulent kinetic energy.

2.2 Species Transport and Discrete Phase Model

Inlet diffusion and diffusion energy source were selected for the species transport. The net transport of species at inlets was computed using a pressure-based solver, accounting for both the convection and diffusion components. The convection components were fixed by the user's input species mass percentage, whereas the diffusion component was dependent on the gradient of the predicted species field at the inlet. The discrete particle model (DPM) was used to capture the atomization phase and the flow of vapour formation. The particle tracking methods used were interaction with continuous particles, unsteady particle tracking, and tracking with fluid flow time steps. The continuing phase, in which

the force balance on the particle was integrated into the solver to determine the particle trajectories, was calculated by solving the Navier-Stokes equations and the continuity equation. The continuous phase in the event of a two-way interaction was computed using the Eulerian Model. Integrating the force balance on the particle, which is expressed in a Lagrangian reference frame, yields the track of a discrete phase particle.

2.3 Spray and Breakup Simulation

The fuel injection development involved processes such as spray breaking up, atomization, and evaporation. There are two stages for the breakup process: the initial breakup and the secondary breakup. In the current simulation, the first drops of atomized fuel were created near the nozzle exit. The secondary process picked up where the initial small droplets continuously atomized into smaller droplets.

2.3.1 *Primary Breakup*

The main breakup model concept follows the KH-RT breakup model concept, as shown in Figure 2 as published by Ishak *et al*. [17]. The aerodynamic forces produced by Kelvin-Helmholtz (KH) waves and Rayleigh-Taylor (RT) instabilities that induce secondary breakup are combined to form the model for the main breakup. Due to KH instability, the droplet splits apart near the nozzle exit in region A. At the same time, the secondary breakdown in region B is brought on by the RT instability.

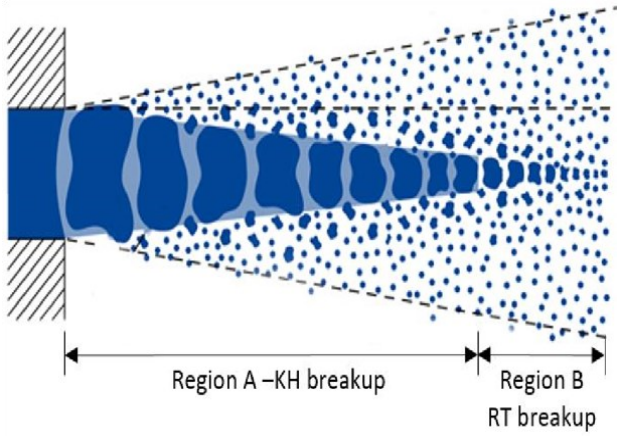

Figure 2. KH-RT breakup model concept (reproduced from Ishak et al. (2019) [17], under the terms of the Creative Commons Attribution 4.0 License)

2.3.2 *Secondary Breakup*

To depict the combination of the spray process's aerodynamic mechanism, the secondary breakup model was constructed. The Stokes number (Stk) is one of the factors that has the most impact on how discrete particles behave in a continuous-phase medium, as shown in Equation (1).

$$Stk = \frac{t_0 u_0}{l_0} \tag{1}$$

Where u_0 is the initial flow velocity, l_0 is the characteristic diameter of the obstacle, and t_0 is the particle relaxation time. At first, the discrete particles followed their initial trajectories due to the high Stokes number. Due to decreasing Stoke number values, the discrete particles were thereafter maintained on their fluid streamlines. Therefore, more tiny particles were produced during the breakup process when the Stoke number was lower. The commonly used Taylor analogy breakup (TAB) was utilised in this study to take these breakup forces into consideration. It was based on Taylor's comparison of a spring-mass system and an oscillating and deforming droplet.

2.4 Sauter Mean Radius

By converting the energy of the parent droplet to the sum of the energies of the child droplets, the size of the child droplets can be determined. Based on an analysis of the energy conversion between a parent and child droplet, the Sauter mean radius of the product droplet can be determined by setting as follows:

$$r_{32} = \frac{r}{1 + \frac{8Ky^2}{20} + \frac{\rho_l r^3 (dy/dt)^2}{\sigma}\left(\frac{6K-5}{120}\right)} \tag{2}$$

Where r_{32} is the Sauter mean radius of the droplet size distribution, r is the undisturbed droplet radius, K is the ratio of the total energy in distortion and oscillation to the energy, y is the wall distance in the boundary layer, ρ_l is the discrete phase density, and σ is the droplet surface tension.

2.5 Fuel Properties

The type of fuel used in this study was diesel, palm oil and its blends. The physical properties of the palm oil and its blends are shown in Table 4. The material properties of the diesel are available in the Fluent database, as shown in Table 5. While, for palm oil the properties are based on calculation.

Table 4 Physical properties of PODB [19]

Fuel	Density (kg/m³)	Calorific Value (kJ/kg)	Viscosity (mm²/s)	Molecular weight (kg/kmol)
P20	855	42 840	24.55	283.29
P40	863	41 558	27.32	424.29
P60	882	41 184	45.90	565.29
P80	896	40 165	50.93	706.30
P100	904	39 027	59.68	847.30

Table 5 Material properties of diesel

Fuel	Density (kg/m³)	Surface Tension (N/m)	Molecular weight (kg/kmol)	Viscosity (poise)
Diesel	818.1	0.0264	142.29	0.1395
Palm oil (P100)	904.0	0.0315	847.30	0.5985

3.0 RESULTS AND DISCUSSION

3.1 Model Validation

For the model validation, results from Yu *et al*. [20] and Ishak *et al*. [17] were chosen because of the similarity of the boundary condition that proved each other's results. Results of tip penetration for this simulation compared to the results obtained by Yu *et al*. [20] and Ishak *et al*. [17] are shown in Table 6. The average percentage difference for tip penetration was 8.25 % to 10.64 % compared to the experiment by Yu *et al*. [20] and the simulation by Ishak *et al*. [17], respectively. Overall, the tip penetration trends of this study are similar to those of other researchers.

Table 6 Validation results of tip penetration for diesel fuel and percentage of error

Time (ms)	Penetration length			Percentage of error	
	Yu *et al.* [20]	Ishak *et al.* [17]	Model (This study)	Compare to Yu *et al.* [20]	Compare to Ishak *et al.* [17]
0.2	13.00	11.00	13.96	7.3892	26.915
0.3	16.25	16.25	19.69	21.1385	21.139
0.4	21.00	20.00	23.62	12.4862	18.111
0.5	23.00	22.50	25.59	11.2635	13.736
0.6	27.00	25.00	27.56	2.0707	10.236
0.7	28.50	28.50	29.53	3.6056	3.606
0.8	32.00	30.00	30.32	5.2656	1.050
0.9	32.50	30.50	30.71	5.5117	0.684
1.0	35.00	33.00	33.08	5.4780	0.251
			Error (%)	8.2454	10.636

3.2 Spray Characteristics of Palm Oil Diesel Blend Ratio

Both macroscopic and microscopic parameters of fuel spray were investigated for all fuels (diesel, P20, P40, P60, P80, and P100). The macroscopic parameters, such as tip penetration and cone angle, were measured directly from the spray images, while the microscopic parameter, which was the Sauter mean diameter, was obtained from the analysis report. At the beginning, the characteristics of pure palm oil spray were compared to diesel. Palm oil has the highest density, surface tension, and molecular weight compared to diesel. Figure 3 shows the spray development of palm oil and diesel at 0.2 to 0.6 ms after the start of injection (ASOI). The longer tip penetration was observed for palm oil compared to diesel. In terms of cone angle, it showed that diesel had produced a larger cone angle compared to palm oil. These findings confirmed the physical properties affected the fuel spray process; thus, further quantitative analysis was conducted based on tip penetration, cone angle, and Sauter mean diameter.

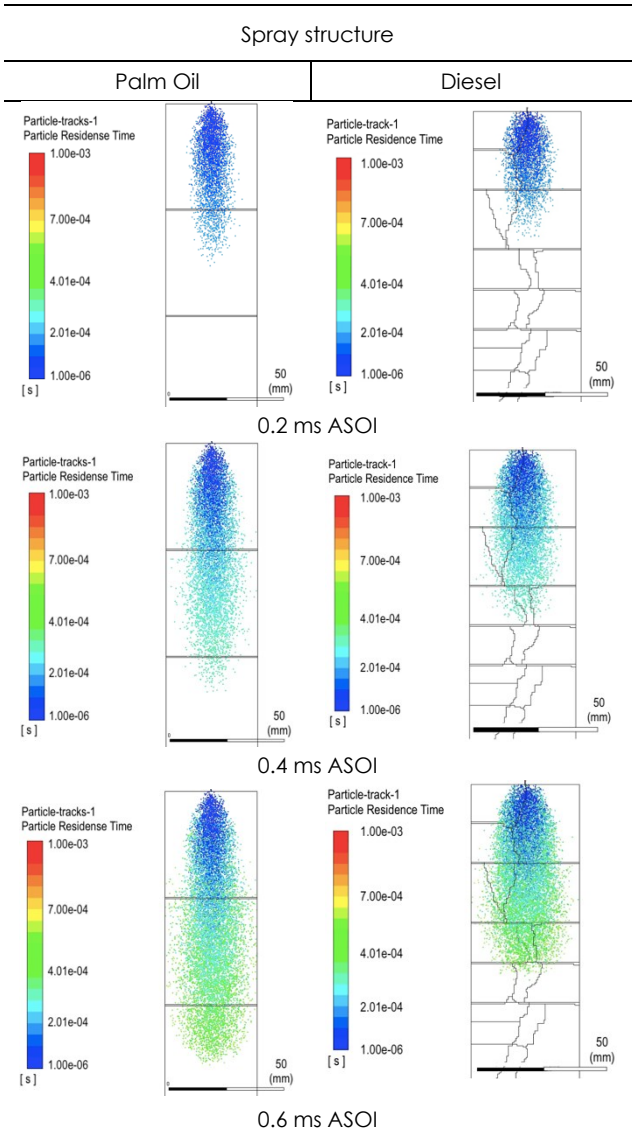

Figure 3 Spray structure of diesel and palm oil (100 %) at 160 MPa injection pressure

Figure 4 shows a comparison of tip penetration for palm oil diesel blends to diesel at a standard nozzle size (0.18 mm) and injection pressure of 160 MPa. The palm oil was blended with diesel at various volume percentages, which were 20, 40, 60, 80, and 100 % (pure palm oil), identified as P20, P40, P60, P80, and P100, respectively. The tip penetration for all fuels increased with time, and the tip penetration pattern agreed well with other researchers' studies [17], [20], [21]. As the injection progressed, the tip penetration of palm oil and its blends was longer compared to diesel,

indicating that they developed faster compared to the spray development of diesel. Further observation found that P100 had the longest tip penetration, followed by P80, P60, P40, and P20. The shortest tip penetration was produced by diesel fuel. This behaviour might happen due to the higher density, surface tension, and viscosity for palm oil and its blends. The viscosity of palm oil was about 59.68 mm^2/s, which was much higher compared to diesel, which was about 13.95 mm^2/s only, while the molecular weight of palm oil was 847.3 kg/kmol compared to diesel's 142.29 kg/kmol. These properties had caused higher spray tip penetration for palm oil in spray breakup, resulting in more spray development along the axial direction rather than the radial direction [22]. The experimental studies by other researchers had also found the high-density and viscosity fuel would produce the highest tip penetration [11], [21], [23], [24]. Lee *et al*. [25] had experimentally investigated the spray characteristics of karanja biodiesel and its blends with diesel, and it was found that at lower injection pressure, higher density, and viscosity, the fuel (karanja fuel) would produce lower tip penetration compared to diesel. However, at higher injection pressure (more than 50 MPa), higher tip penetration was produced by the higher density and viscosity fuel (karanja fuel).

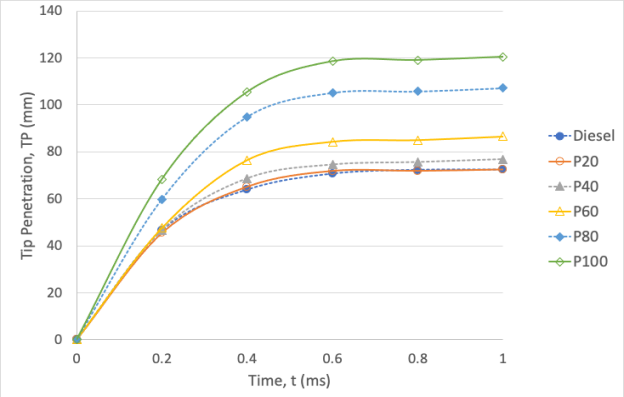

Figure 4 Comparison of tip penetration for all PODB to diesel at nozzle size 0.18 mm and injection pressure of 160 MPa

Faster tip penetration and a wider cone angle will demonstrate better fuel evaporation [26]. With better fuel evaporation, it will contribute to a better air-fuel mixing process. Figure 5 shows the comparison of the cone angle for PODB to diesel fuel at a 0.18 mm nozzle size and an injection pressure of 160 MPa. The cone angle for both fuels was found to be almost constant after the early spray development, in agreement with the same results by Delacourt *et al*. [15]. The highest cone angle was produced by diesel fuel, followed by P20, P40, P60, P80, and P100. P20 had also shown an almost identical cone angle when compared to diesel. The average percentage difference between diesel and all blends was found to be 6.96, 22.28, 38.68, 53.19, and 56.53 % for P20, P40, P60, P80, and P100, respectively. The lowest percentage difference for P20 was probably due to its lower value of viscosity when compared to other blends. A lower value of viscosity would improve the spray breakup process and ensure a wider cone angle for P20. The main reason for this behaviour was the higher viscosity and surface tension of palm oil that contributed to the spray development being more on the axial direction. The cone angle was highly affected by the spray breakup process, and its difficulties produced a narrower cone angle. These findings are consistent with the experimental studies conducted by various researchers. They found that higher density, viscosity, and surface tension fuels would produce narrower spray cone angles [11], [21], [23], [24], [25].

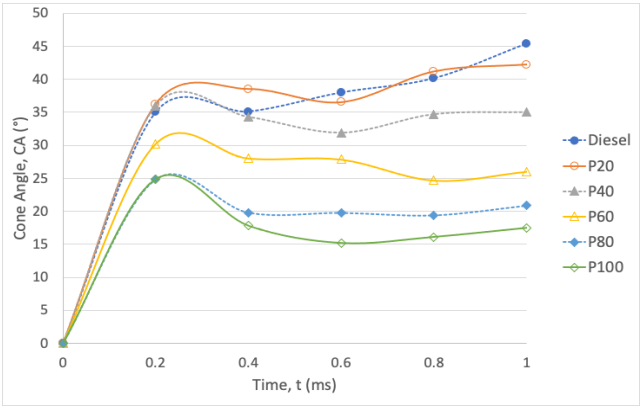

Figure 5 Comparison of cone angle for PODB at 0.18 mm nozzle size and injection pressure of 160 MPa

The SMD value will represent the mean droplet size, and it is one of the microscopic parameters that indicate the quality of spray atomization and the air-fuel mixing process. Smaller droplet size is desired, as it will increase the area of fuel in contact with air, and smaller droplet size is easier to evaporate compared to a large droplet size [21]. The comparison of SMD for PODB to diesel fuel at a 0.18 mm nozzle size and injection pressure of 160 MPa is shown in Figure 6. It was found that the SMD of the fuel spray increased with the increasing of palm oil volume in the blended fuel. The smallest droplet size for PODB was produced by P20, followed by P40, P60, P80, and P100. The percentage of difference of SMD compared to diesel for all blends was at about 20.75, 37.98, 108.66, 174.36, and 238.98 % for P20, P40, P60, P80, and P100, respectively. Once again P20 had shown the closest spray characteristics when compared to diesel. This trend can be traced back to the less restrictive flow of fuel through the nozzle, making its velocity faster and able to break up into smaller particles. The fuel viscosity and surface tension had affected the mean droplet size, whereas high viscosity and surface tension fuel would produce larger SMD [21].

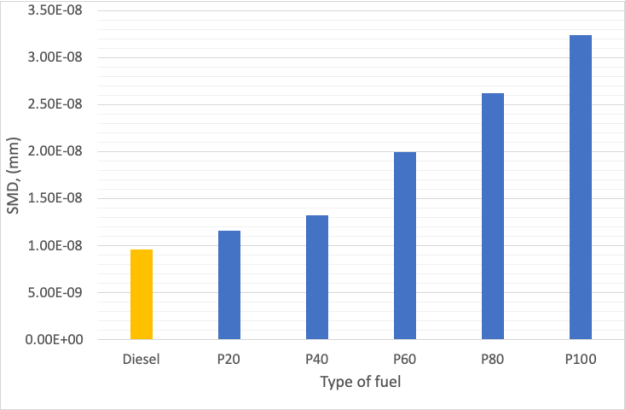

Figure 6 Comparison of SMD for PODB at 0.18 mm nozzle size and injection pressure of 160 MPa

3.3 Effect of Different Injection Pressures

This study also investigated the effects of injection pressure. Injection pressure employed for this simulation analysis was in between 120 and 200 MPa. The tip penetration, cone angle, and SMD comparison for PODB are shown in Figures 7, 8, and 9, respectively. Although all PODB were tested, only the P20, P60 and P100 results are shown. Analysis has shown that the tip penetration will increase with the increasing injection pressure. Increasing the injection pressure to 200 MPa would produce longer average tip penetration at about 11.01, 11.99, 16.55, 14.36, and 11.60 % for P20, P40, P60, P80, and P100, respectively.

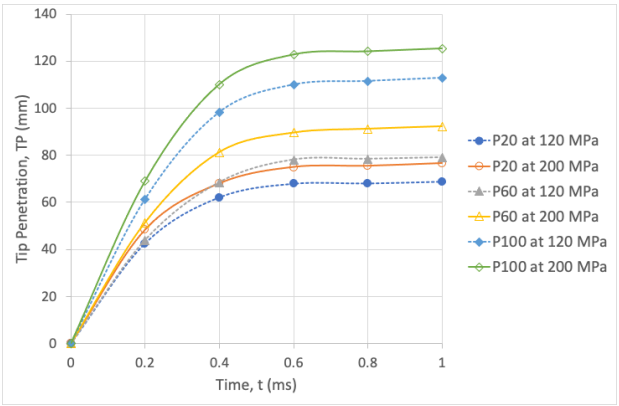

Figure 7 Comparison of tip penetration for P20, P60 and P100 at various injection pressure and nozzle size of 0.18 mm

The effect of injection pressure on cone angle is shown in Figure 8 for P20, P60, and P100. The fuels were tested at various injection pressures that are 120 to 200 MPa. From the analysis, it was found that the average cone angle improvement was at about 7.27 % for P20 for higher injection pressure. However, for other blends, the average cone angle degraded at about 4.82, 6.17, 10.91, and 0.91 % for P40, P60, P80, and P100, respectively. Comparing the average cone angle for all blends to the diesel average cone angle as the selected standard configuration (injection pressure of 160 MPa), it was found that the P20 and P40 had produced wider cone angles at about 21.89 and 5.70 %, respectively. Meanwhile, narrower cone angles were still produced by P60, P80, and P100, at about 16.09, 37.18, and 44.79 % compared to diesel. A slight improvement on cone angle may contribute to better fuel combustion, although the injection pressure did not show drastic spray characteristics on cone angle.

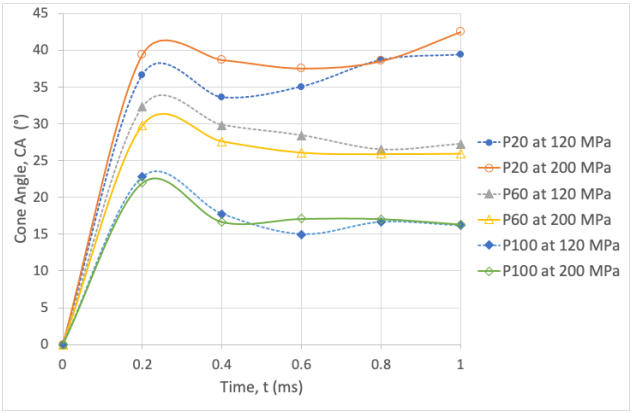

Figure 8 Cone angle comparison for P20, P60 and P100 at different injection pressure and nozzle size of 0.18 mm

The comparison of SMD for PODB at different injection pressures to diesel fuel at the selected datum condition (red line) is shown in Figure 9. Based on the analysis, it was found that the droplet size of the fuel spray increased with increasing palm oil volume in the blended fuel. The smallest droplet size was produced by P20, followed by P40, P60, P80, and P100. At higher injection pressure, the SMD was reduced at about 42.92, 44.25, 39.40, 38.81, and 38.62 % for P20, P40, P60, P80, and P100, respectively. Comparing the SMD at higher injection pressure with diesel at standard configuration, it was found that P20 had produced smaller SMD compared to diesel at about 8.55 %. For other blends, the SMD was still larger, which was at about 5.92, 67.48, 121.07 and 173.44 % when compared to diesel at 160 MPa. Although the SMD for other blends remained larger than that of diesel, increasing the injection pressure would enhance the droplet size.

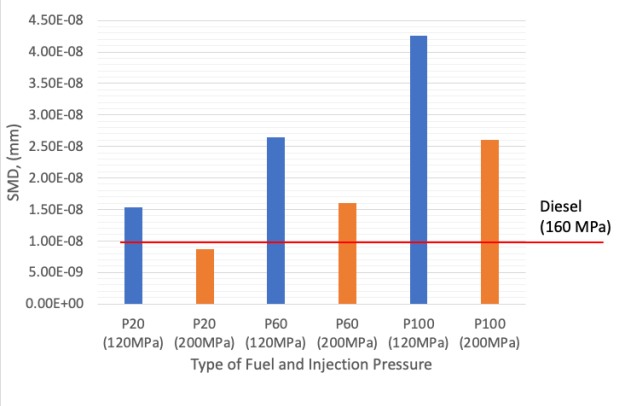

Figure 9 SMD comparison for P20, P60 and P100 at different injection pressure

3.4 Effect of Nozzle Size

Since the spray characteristics and SMD were improved at higher injection pressure, further investigation on the effect of nozzle size was conducted at 200 MPa injection pressure. The PODB was tested at various nozzle sizes from 0.14 to 0.22 mm. Figure 10 shows the comparison of PODB tip penetration at 0.14 and 0.22 mm nozzle sizes and 200 MPa injection pressure. Based on the results, it was found that the tip penetration for all blends increased with the increasing of the nozzle size. For all blends, a nozzle size of 0.22 mm had produced the longest tip penetration. The percentage of tip penetration increase when a 0.22 mm nozzle size is used is at about 18.78, 31.67, 43.15, 46.40, and 45.27 % for P20, P40, P60, P80, and P100, respectively. From these findings, it can be concluded that the largest nozzle size and highest density fuel would produce the longest tip penetration, and it may improve one side of the spray characteristics.

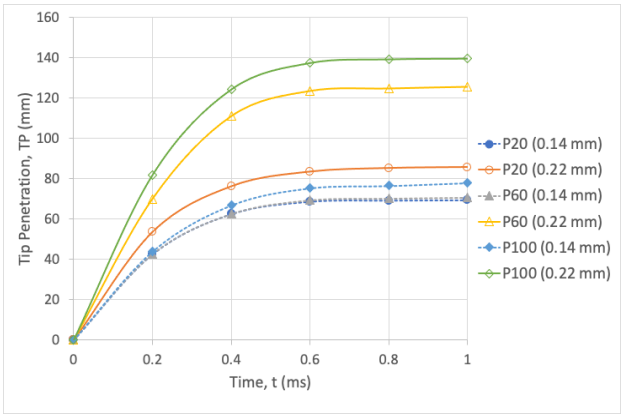

Figure 10 Comparison of P20, P60 and P100 at various nozzle size and injection pressure of 200 MPa

Figure 11 shows the comparison of cone angles of all blends at 0.14 and 0.22 mm nozzle sizes for P20, P60, and P100. From the analysis, it was found that P20 had improved by 5.89 % with the usage of a larger nozzle size. However, for other blends, the cone angles were narrower at about 7.55, 16.01, 49.47, and 45.48 % for P40, P60, P80, and P100, respectively. The main reason to the smaller cone angle for PODB was most probably due to faster tip penetration, which would affect the development of spray in an axial rather than radial direction. Comparing the results at 200 MPa and 0.22 mm nozzle size with diesel at standard configuration, it was found that only P20 had improved on the cone angle by 15.46 %, while for other blends, the cone was still smaller compared to diesel at about 28.67, 63.09, 113.65, and 130 % for P40, P60, P80, and P100, respectively.

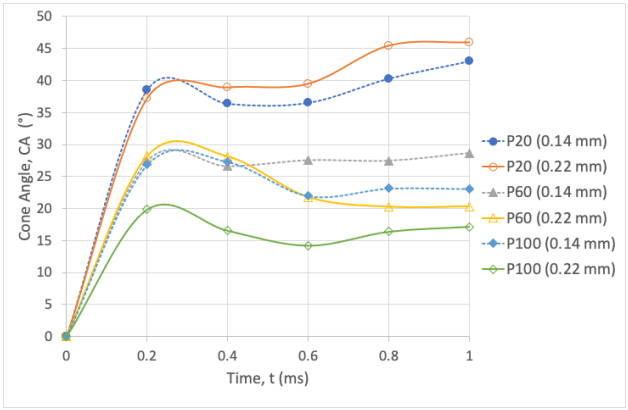

Figure 11 Comparison of cone angle for P20, P60 and P100 at various nozzle size and injection pressure of 200 MPa

Figure 12 shows the comparison of SMD for PODB at 0.22 mm nozzle sizes and an injection pressure of 200 MPa. In general, the SMD decreases with the increasing nozzle size to about 46.59, 13.29, 18.81, 17.30, and 26.43 % for P20, P40, P60, P80, and P100, respectively, when compared to PODB injected using a 0.18 mm nozzle size and 180 MPa injection pressure. Comparing the SMD for blends to diesel at standard injection configuration, it was found that P20 had produced a smaller SMD at about 35.51 % compared to diesel. However, for P40, P60, P80, and P100 the blends had produced larger SMD at about 19.65, 69.41, 126.91, and 149.38 %, respectively, compared to diesel. Even though the SMD for other blends was still larger compared to diesel, the values were significantly reduced with the larger nozzle size and higher injection pressure.

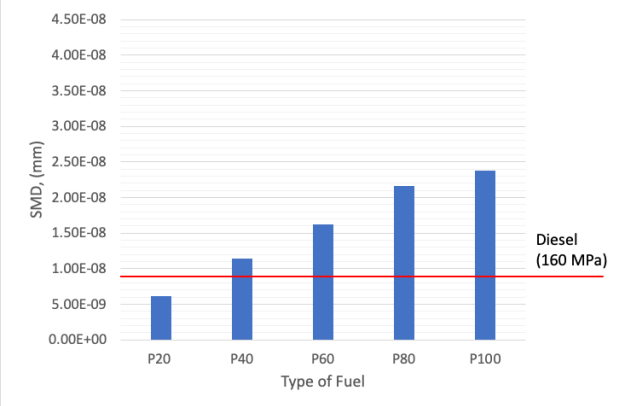

Figure 12 Comparison of droplet size for P20, P40, P60, P80 and P100 at 0.22 mm nozzle size and injection pressure of 200 MPa

Based on spray characteristics analysis at various PODB ratios, injection pressures, and nozzle sizes, it revealed various information on tip penetration, cone angle, and SMD. Higher injection pressure and larger nozzle size would improve the spray characteristics, especially for tip penetration and SMD. The aim of the study is to find the optimised configuration for PODB that can match with diesel at the selected standard configuration. It was found that the tip penetration and SMD will significantly improve with higher injection pressure and larger nozzle size.

Table 7 Suggested configuration of injection pressure and nozzle size for each blend and percentage different compared to diesel.

Fuel	Injection pressure (MPa)/ Nozzle Size (mm)	Average tip penetration / % different	Average cone angle / % different	SMD / % different
Diesel	160/ 0.18	65.10 mm / -	38.71° / -	9.55 x 10^{-9} mm / -
P20	200/ 0.22	77.00 mm / 15.46 % longer	41.40° / 6.50 % wider	6.16 x 10^{-9} mm / 35.51 % smaller
P40	200/ 0.20	91.48 mm / 28.84 % longer	30.08° / 28.67 % narrower	1.14 x 10^{-8} mm / 19.65 % larger
P60	200/ 0.20	111.07 mm / 41.38 % longer	23.74° / 63.09 % narrower	1.62 x 10^{-8} mm / 69.41 % larger
P80	200/ 0.20	117.27 mm / 44.49 % longer	18.12° / 113.66 % narrower	2.17 x 10^{-8} mm / 126.91 % larger
P100	200/ 0.20	124.61 mm / 47.76 % longer	16.82° / 130.10 % narrower	2.38 x 10^{-8} mm / 149.38 % larger

However, in terms of cone angle, only P20 can supersede the cone angle of diesel at standard configuration. For other blends, the cone angle improved, but it was still lower compared to diesel. The suggested configuration for each blend is shown in Table 7.

4.0 CONCLUSION

The macroscopic and microscopic spray characteristics of PODB and the effect of blend ratio, nozzle size, and injection pressure were successfully studied. The model of fuel injection spray based on the diesel injector system has been developed using Ansys Fluent software, and the percentage of error was found to be 8.25 % and 10.64 % compared to experimental and simulation studies, respectively.

A parametric study on different blend ratios, nozzle sizes, and injection pressures shows that higher injection pressures result in longer tip penetration and smaller SMD. Meanwhile, increasing the nozzle size also will produce longer tip penetration and smaller droplet size. The most identical blend to diesel is P20. As for the other blends, the spray characteristics can be improved by using higher injection pressure, which is at 200 MPa.

The tip penetration, cone angle, and droplet size were significantly improved at higher injection pressure and larger nozzle size. The injection pressure and nozzle size were suggested to be increased by about 25 % from the standard condition for diesel. Altering the injection timing was also suggested for higher injection pressure for PODB to avoid wall impingement.

Acknowledgement

The authors thank the Ministry of Higher Education (MOHE), Malaysia for the financial support provided via the Fundamental Research Grant Scheme [ref no FRGS/1/2019/TK03/UNIKL/01/2]. The authors also thank Universiti Kuala Lumpur, Malaysia for the support provided via UniKL-UERGS Grant [ref no UER24010], and UniKL Malaysian Spanish Institute for providing necessary facilities and resources to complete this study for publication.

Conflicts of Interest

The authors declare that there is no conflict of interest regarding the publication of this paper.

References

[1] Shervani-Tabar, M. T., M. Sheykhvazayefi, and M. Ghorbani. 2013. Numerical Study on the Effect of the Injection Pressure on Spray Penetration Length. *Applied Mathematical*

Modelling. 37(14–15): 7778–7788. https://doi.org/10.1016/J.APM.2013.03.002.
[2] Soid, S. N., and Z. A. Zainal. 2011. Spray and Combustion Characterization for Internal Combustion Engines Using Optical Measuring Techniques – A Review. *Energy*. 36(2): 724–741. https://doi.org/10.1016/j.energy.2010.11.022.
[3] Agarwal, A. K., et al. 2018. Review of Experimental and Computational Studies on Spray, Combustion, Performance, and Emission Characteristics of Biodiesel Fueled Engines. *Journal of Energy Resources Technology*. 140(12). https://doi.org/10.1115/1.4040584.
[4] Senthil, R., and G. A. Vijay. 2023. Review of Physicochemical Properties and Spray Characteristics of Biodiesel. *Environmental Science and Pollution Research*. 30(25): 66494–66513. https://doi.org/10.1007/s11356-023-27250-4.
[5] Mehra, K. S., J. Pal, and V. Goel. 2023. A Comprehensive Review on the Atomization and Spray Characteristics of Renewable Biofuels. *Sustainable Energy Technologies and Assessments*. 56: 103106. https://doi.org/10.1016/j.seta.2023.103106.
[6] Suhara, A., et al. 2024. Biodiesel Sustainability: Review of Progress and Challenges of Biodiesel as Sustainable Biofuel. *Clean Technologies*. 6(3): 886–906. https://doi.org/10.3390/cleantechnol6030045.
[7] Feng, Z., C. Zhan, C. Tang, K. Yang, and Z. Huang. 2016. Experimental Investigation on Spray and Atomization Characteristics of Diesel/Gasoline/Ethanol Blends in High Pressure Common Rail Injection System. *Energy*. 112. https://doi.org/10.1016/j.energy.2016.06.131.
[8] Andsaler, A. R., A. Khalid, N. S. Adila Abdullah, A. Sapit, and N. Jaat. 2017. The Effect of Nozzle Diameter, Injection Pressure and Ambient Temperature on Spray Characteristics in Diesel Engine. *Journal of Physics: Conference Series*. https://doi.org/10.1088/1742-6596/822/1/012039.
[9] Tang, C., Z. Feng, C. Zhan, W. Ma, and Z. Huang. 2017. Experimental Study on the Effect of Injector Nozzle K Factor on the Spray Characteristics in a Constant Volume Chamber. *Fuel*. 202. https://doi.org/10.1016/j.fuel.2017.04.078.
[10] Payri, R., J. P. Viera, V. Gopalakrishnan, and P. G. Szymkowicz. 2017. The Effect of Nozzle Geometry over the Evaporative Spray Formation for Three Different Fuels. *Fuel*. 188. https://doi.org/10.1016/j.fuel.2016.10.064.
[11] Ma, Y., S. Huang, R. Huang, Y. Zhang, and S. Xu. 2017. Ignition and Combustion Characteristics of n-Pentanol–Diesel Blends in a Constant Volume Chamber. *Applied Energy*. 185. https://doi.org/10.1016/j.apenergy.2016.11.002.
[12] Lee, M. Y., G. S. Lee, C. J. Kim, J. H. Seo, and K. H. Kim. 2018. Macroscopic and Microscopic Spray Characteristics of Diesel and Gasoline in a Constant Volume Chamber. *Energies*. 11(8). https://doi.org/10.3390/en11082056.
[13] Yamaguchi, A., L. Koopmans, A. Helmantel, F. P. Karrholm, and P. Dahlander. 2019. Spray Characterization of Gasoline Direct Injection Sprays under Fuel Injection Pressures up to 150 MPa with Different Nozzle Geometries. *SAE Technical Papers*. https://doi.org/10.4271/2019-01-0063.
[14] Wang, X., Z. Huang, W. Zhang, O. A. Kuti, and K. Nishida. 2011. Effects of Ultra-High Injection Pressure and Micro-Hole Nozzle on Flame Structure and Soot Formation of Impinging Diesel Spray. *Applied Energy*. 88(5). https://doi.org/10.1016/j.apenergy.2010.11.035.
[15] Delacourt, E., B. Desmet, and B. Besson. 2005. Characterisation of Very High Pressure Diesel Sprays Using Digital Imaging Techniques. *Fuel*. 84(7–8). https://doi.org/10.1016/j.fuel.2004.12.003.
[16] Khalid, A., *et al*. 2017. Computational Fluid Dynamics Analysis of High Injection Pressure Blended Biodiesel. *IOP Conference Series: Materials Science and Engineering*. https://doi.org/10.1088/1757-899X/226/1/012002.
[17] Ishak, M. H. H., F. Ismail, S. C. Mat, M. Z. Abdullah, M. S. Abdul Aziz, and M. Y. Idroas. 2019. Numerical Analysis of Nozzle Flow and Spray Characteristics from Different Nozzles Using Diesel and Biofuel Blends. *Energies*. 12(2). https://doi.org/10.3390/en12020281.
[18] Kafrawi, F., K. H. Lee, C. Zhang, and S. Bari. 2022. Spray Analysis of Palm-Based Biodiesel to Correlate Performance and Combustion Analysis of a Compression Ignition Engine. *Fuel*. 319. https://doi.org/10.1016/j.fuel.2022.123822.
[19] Soid, S. N., Z. A. Zainal, M. A. Iqbal, and M. A. Miskam. 2012. Macroscopic Spray Characteristics of Palm Oil–Diesel Blends in a Constant Volume Combustion Chamber. *Journal of Scientific and Industrial Research*. 71: 740–747.
[20] Yu, S., *et al*. 2018. Experimental Study on the Spray Characteristics Discharging from Elliptical Diesel Nozzle at Typical Diesel Engine Conditions. *Fuel*. 221. https://doi.org/10.1016/j.fuel.2018.02.090.
[21] Bhikuning, A., E. Matsumura, and J. Senda. 2018. A Review: Non-Evaporating Spray Characteristics of Biodiesel Jatropha and Palm Oil and Its Blends. https://doi.org/10.15866/ireme.v12i4.14037.
[22] Han, D., J. Zhai, Y. Duan, D. Ju, H. Lin, and Z. Huang. 2017. Macroscopic and Microscopic Spray Characteristics of Fatty Acid Esters on a Common Rail Injection System. *Fuel*. 203: 370–379. https://doi.org/10.1016/j.fuel.2017.04.098.
[23] Deng, J., C. Li, Z. Hu, Z. Wu, and L. Li. 2010. Spray Characteristics of Biodiesel and Diesel Fuels under High Injection Pressure with a Common Rail System. *SAE Technical Papers*. https://doi.org/10.4271/2010-01-2268.
[24] Zhan, C., Z. Feng, W. Ma, M. Zhang, C. Tang, and Z. Huang. 2018. Experimental Investigation on Effect of Ethanol and Di-Ethyl Ether Addition on the Spray Characteristics of Diesel/Biodiesel Blends under High Injection Pressure. *Fuel*. 218. https://doi.org/10.1016/j.fuel.2017.12.038.
[25] Lee, S., C. S. Lee, S. Park, J. G. Gupta, R. K. Maurya, and A. K. Agarwal. 2017. Spray Characteristics, Engine Performance and Emissions Analysis for Karanja Biodiesel and Its Blends. *Energy*. 119. https://doi.org/10.1016/j.energy.2016.12.043.
[26] Gao, J., D. Jiang, and Z. Huang. 2007. Spray Properties of Alternative Fuels: A Comparative Analysis of Ethanol–Gasoline Blends and Gasoline. *Fuel*. 86(10–11). https://doi.org/10.1016/j.fuel.2006.11.013.